Case Studies in Thermal Engineering 25 (2021) 100867

Contents lists available at ScienceDirect

Case Studies in Thermal Engineering

journal homepage: http://www.elsevier.com/locate/csite

Numerical computation of buoyancy and radiation effects on MHD micropolar nanofluid flow over a stretching/shrinking sheet with heat source

Saif Ur Rehman [a], Amna Mariam [b], Asmat Ullah [b], Muhammad Imran Asjad [a], Mohd Yazid Bajuri [c], Bruno A. Pansera [d], Ali Ahmadian [e,*]

[a] Department of Mathematics, University of Management and Technology, Lahore, Pakistan
[b] School of Mathematics, National College of Business Administration and Economics Lahore Layyah Campus, By Pass Road, Layyah, Pakistan
[c] Department of Orthopaedics and Traumatology, Faculty of Medicine, Universiti Kebangsaan Malaysia(UKM), Kuala Lumpur, Malaysia
[d] Decisions Lab, Mediterranea University of Reggio Calabria, Reggio Calabria, 89125, Italy
[e] Institute of IR 4.0, The National University of Malaysia, UKM Bangi, 43600, Selangor, Malaysia

ARTICLE INFO

Keywords:
Radiation
Buoyancy parameters
Micro-polar fluid
Magnetohydrodynamics
Nano-fluid
Heat source

ABSTRACT

In this mathematical study, the effect of buoyancy parameters along with radiation on magneto-hydrodynamic (MHD) micro-polar nano-fluid flow over a stretching/shrinking sheet is taken into consideration. Suitable similarity variables are used to convert the governing non-linear partial differential equations into a system of coupled non-linear ordinary differential equations which are then numerically solved by R.K method with shooting scheme. The influence of pertinent parameters on the velocity profile, temperature profile, micro-rotation profile, and concentration profile is investigated. It is founded that the velocity profile is decreased with the increment in the values of M and the opposite behavior is noticed for micro-rotation, thermal, and concentration profiles. It is also founded that an increase in the values of buoyancy parameters causes an increase in velocity profile while micro-rotation, thermal, and concentration profiles are decreased. The results are exposed and discussed through tables and graphs.

1. Introduction

Nanofluids contain nanosize metallic structures diffused with the base fluid. Commonly these tiny particles are constructed by carbides, oxides, metals etc. The properties of these tiny objects are very real which makes them likely valuable in applications of heat transfer. It is difficult to decide the appropriateness of the rheological attitude of nano-fluids for convective heat transfer applications. Xie et al. [1] studied Electro kinetic energy conversion of nanofluids in MHD-based microtube. Over a heated inclined plate, Mitra [2] discussed the nano-fluids flow with the computational modeling. Chakraborty [3] discussed the nano-fluids with radiations. On a passable sheet, Ziaei-Rad et al. [4]. elaborated the nano-fluids flow along with the similarity solutions. Mebarek-Oudina et al. [5]. worked on the heat transfer of nano-fluids. Raza et al. [6] discussed the effects of nano-fluid flow along with the effect of multiple slips over a permeable sheet.

Micro-polar is one of the best concepts which is suggested for structured fluids. It contains tiny structures that can not be seen from

* Corresponding author.
E-mail address: ali.ahmadian@ukm.edu.my (A. Ahmadian).

https://doi.org/10.1016/j.csite.2021.100867
Received 14 October 2020; Received in revised form 16 January 2021; Accepted 27 January 2021
Available online 4 March 2021

a common eye. Many fluids flow has been observed several times to find the change of these micro-structures. They associate the fluids which have unbalanced stress tensor, called polar fluids. They also include a particular case that is the Navier-stokes model in classical fluids. In the area of research the theory of micro-polar fluids has become very popular. With the help of micro-polar theory many researchers are committed to showing helpful results. Kumar et al. [7] discussed the stream of MHD of micropolar liquid due to permeable surface with viscous dissipation in the presence of improved heat flux model. With the numerical study, Anwar et al. [8] explained the outflow of micro-polar nano-fluid with a stretching layer. Kumar et al. [9] presented thermophoresis Brownian motion influence of Magnetohydrodynamics micropolar nanofluid stream over extending sheet having the non-uniform source of heat. Anantha et al. [10] discussed physical effect on Magnetohydrodynamics micropolar fluid stream through an exponentially extending Curved sheet. Yacob et al. [11] explained many forms of the micro-polar fluid flow. Kumar at al [12]. presented a non-Fourier heat flux model for MHD micropolar liquid flow across a coagulated sheet.

The main concept of the magneto-hydrodynamic, is that in a moving conductive field, magnetic field creates a current which construct forces and itself adjusts the magnetic field. Magneto-hydrodynamic discusses the difficult relation between plasma and magnetic fields, which are liable for many dynamic actions in many immense objects including the sun. MHD has an influence in the developments of selenology that is magnetic flux emergence, burning, concentration on the production of magnetic fields. In many engineering and industrial processes along with geophysics and astrophysics the boundary layer flow of magnetic-hydrodynamic for incompressible and electrically conducting fluids is encountered. Which plays an important role in electronics, chemical engineering, metallurgy, meteorology. Kasiviswanathan et al. [13] get feasible solutions for the magneto-hydrodynamic flow of micro-polar liquid which is confined between two similar, insulated, endless, non-coaxially pivoting disks. With an inclined sheet, Khan [14] elaborated the transfer of mass and heat of magnetic-hydrodynamic flow of nano-fluids. Anantha et al. [15] discussed physical effect on unsteady magnetohydrodynamics stagnation point flow at free convective through extending sheet. Tlili et al. [16] introduced the aspect of asymmetrical film flow on MHD hybrid ferrofluid having variable heat. Kempannagari et al. [17] introduced MHD stream of non-Newtonian liquid due to vertically permeable curved sheet by considering the influence of joule heating. Kumar et al. [18] discussed the influence of magnetohydrodynamics Casson fluid stream through vertically extending curved surface having thermal radiation. Ahmed et al. [19] analyzed MHD natural convection from two heating modes in fined triangular enclosures filled with porous media using nanofluids. Anwar et al. [20] analyzed an exact analysis of unsteady MHD free convection flow of some nanofluids with ramped wall velocity and ramped wall temperature accounting heat radiation and injection/consumption. Hassan [21] considered the electrically conducting viscous boundary layer flow and heat transfer. Anantha et al. [22] presented MHD Cattaneo-Christove through variable heat source/sink. Nadeema et al. [23] worked on micro-hydrodynamics flow over a shrinking sheet. Ramadevi et al. [24] Studied the influence of non-uniform heat source/sink on the three-dimensional magnetohydrodynamic Carreau fluid flow past a stretching surface with modified Fourier's law. Kumar et al. [25] analyzed the magnetohydrodynamic carreau fluid stream over a melting surface with cattaneo-christov heat flux. By assimilating the heat source, Thumma et al. [26] worked on the flow of magneto-hydrodynamic nano-fluids. Aman et al. [27] discussed the effect of MHD on the flow of nano-fluid which is a non-Newtonian fluid.

The radiation word is proceeds from the process of waves radiating that is moves in all directions. Basically, radiations are called the energy moving from one place to another in waveform. Radiations can be classified by ionizing or non-ionizing which are dependent on the objects that are radiated. These radiations spread when these travel through a region of space. By using a slanted sheet, Govindarajan [28] worked on nano-fluid flow. Anantha et al. [29] introduced effect of thermophoresis and browninan motion on stream of nanoliquids due to bioconvective through variable thickness surface having influence of slip. Venkata et al. [30] presented the heat and mass transfer in MHD Casson nanofluid flow past a stretching sheet with thermophoresis and Brownian motion. With the addition of nano-particles, Mabood et al. [31] worked on it with the increase in thermal conductivity. Rashidi [32] discussed the MHD mixed convective heat transfer for a laminar, incompressible, and a viscoelastic fluid outflow in which electricity can pass. Anantha et al. [33] introduced stream of micropolar liquid for first and second order slip through a convective surface having source of variable heat and Lorentz force for simultaneous solutions. By using the stretching/shrinking sheet, Khan et al. [34] explained the effect on the flow of nano-fluid along with the radiation.

Sakiadis [35] initiated the study of boundary layer flow having the same velocity on a stable surface of solid. Mahapatra et al. [36] studied numerically magneto-hydrodynamic (MHD) with stagnation point flow along with the stretching sheet. Daniel et al. [37] investigate the slip role for unsteady MHD mixed convection of nanofluid over stretching sheet with thermal radiation and electric field. Mabood et al. [38] analyzed the effects of slip and radiation on convective MHD Casson nanofluid flow over a stretching sheet influenced by variable viscosity.

According to the author's best knowledge, there is scanty work to address magneto-hydrodynamic (MHD) micro-polar nano-fluid flow with multiple buoyancies over an extending sheet. This idea is conceived to enhance the heat transfer when nanostructure are diffused in the micropolar based fluid. Moreover, the radiative heat flux also improves the thermal distribution. The results may be used in the cooling of electronics, equipment, and various industrial units. The inclusive physical nature of the specific parameters is inspected through the support of graphs. By using proper similarity transformations, the non-linear partial differential equations are converted in a set that is particularly non-linear ordinary differential equations. The influences of the emerging parameters variate the fluid velocity, temperature, solutal, and nanoparticle volume fraction. In this article, the numerical results are attained by the Runge-Kutta method with a shooting scheme.

2. Mathematical formulation

We assume thermal radiation and buoyancy effect on magnetohydrodynamic micropolar nanofluid transpiration across an extending boundary in the presence of heat source. The sheet velocity is $U(x,t) = ax$, where a is the shrinking/stretching rate along the x-axis. $B(x) = B_0 x^{-1/2}$ is the transverse magnetic field with $B_0 \neq 0$, where B_0 is the magnetic field strength. Where the flow of fluid is restrained by $y > 0$. For fixing an origin and keeping the wall stretched, there must exist two forces that are not only numerically equal but the directions of these forces should be the opposite. The physical flow problem is sketched in Fig. 1.

$$\frac{\partial v}{\partial y}+\frac{\partial u}{\partial x}=0, \tag{1}$$

$$\frac{\partial u}{\partial x}u+\frac{\partial u}{\partial y}v=\frac{\partial^2 u}{\partial y^2}\left(\frac{\mu+k}{\rho}\right)+\frac{\partial N}{\partial y}\frac{k}{\rho}-\frac{\sigma B^2 u}{\rho}+g\beta_T(T-T_\infty)+g\beta_C(C-C_\infty), \tag{2}$$

$$k\left(2N+\frac{\partial u}{\partial y}\right)-\gamma\left(\frac{\partial^2 N}{\partial y^2}\right)=-\rho j\left(u\frac{\partial N}{\partial x}+v\frac{\partial N}{\partial y}\right), \tag{3}$$

$$u\frac{\partial T}{\partial x}+v\frac{\partial T}{\partial y}=\alpha\left(1+\frac{16T_\infty^3\sigma^*}{3k^*k}\right)\frac{\partial^2 T}{\partial y^2}+Q(T-T_\infty)+\tau\left(D_B\frac{\partial C}{\partial y}\frac{\partial T}{\partial y}+\frac{D_T}{T_\infty}\left(\frac{\partial T}{\partial y}\right)^2\right), \tag{4}$$

$$\frac{\partial C}{\partial x}u+\frac{\partial C}{\partial y}v=\frac{\partial^2 C}{\partial y^2}D_B+\frac{D_T}{T_\infty}\frac{\partial^2 T}{\partial y^2}, \tag{5}$$

$$\left.\begin{array}{l} u=b, v=v_1, -n\left(\frac{\partial u}{\partial y}\right)=N, T-T_w(x)=0, C-C_w(x)=0, \quad as \quad y=0. \\ u\to 0, \quad N\to 0, \quad T\to T_\infty, \quad C\to C_\infty \quad as \quad y\to\infty. \end{array}\right\} \tag{6}$$

In the Cartesian Coordinate system, the x-axis is taken in the direction of flow along with the plate with a perpendicular y-axis. A uniform temperature T_w, the surface of the plate is managed and C_w is the nano-particle volume fraction at the surface. Also, T and C are temperature and concentration. D_B and D_T are the coefficients for Brownian diffusion and thermophoresis diffusion respectively. The symbols μ, k, and ρ are the dynamic viscosity, vortex viscosity, and fluid density. N, σ, α, γ and g are micro rotation vector, the electrical conductivity, the thermal diffusivity, the spin gradient viscosity, and the gravity acceleration. Also C, T, β_C, and β_T are solutal concentration, temperature, solutal concentration expansion coefficient, and thermal expansion coefficient. σ^*, Q, and K^* are the Stefan-Boltzmann constant, chemical reaction, and mean absorption constant. Introducing the following similarity transformations:where ψ is the stream function and η is the dimensionless coordinate.

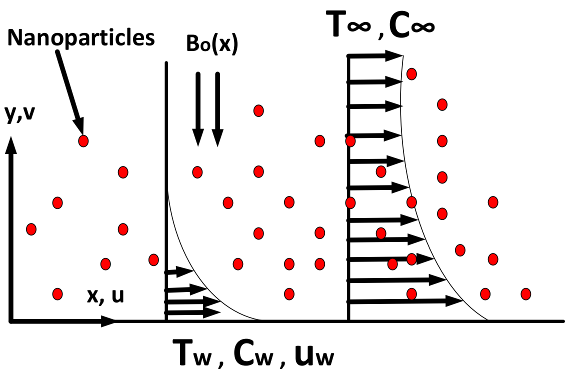

Fig. 1. Flow diagram.

$$\eta=\sqrt{\frac{b}{\nu}}y, \quad \psi=\sqrt{\frac{b\nu}{x}}f(\eta), N=bx\sqrt{\frac{b}{\nu}}g(\eta), \quad \theta(\eta)=\frac{T-T_\infty}{T_w-T_\infty}, \quad \varphi(\eta)=\frac{C-C_\infty}{C_w-C_\infty} \tag{7}$$

In view of Eq. (7), Eqs. (2)–(6) are transformed as under:

$$(K+1)\frac{d^3f}{d\eta^3}-\left(\frac{df}{d\eta}\right)^2+\frac{d^2f}{d\eta^2}f+K\frac{dg}{d\eta}-M\frac{df}{d\eta}+\lambda_1\theta(\eta)+\lambda_2\varphi(\eta)=0, \tag{8}$$

$$\left(1+\frac{K}{2}\right)\frac{d^2g}{d\eta^2}+f\frac{dg}{d\eta}-\frac{df}{d\eta}g-K\left(2g+\frac{d^2f}{d\eta^2}\right)=0, \tag{9}$$

$$\left(\frac{1+R_d}{P_r}\right)\frac{d^2\theta}{d\eta^2}+f\frac{d\theta}{d\eta}+Q'\theta(\eta)+Nb\frac{d\varphi}{d\eta}\frac{d\theta}{d\eta}+Nt\left(\frac{d\theta}{d\eta}\right)^2, \tag{10}$$

$$\frac{d^2\varphi}{d\eta^2}+Lef\frac{d\varphi}{d\eta}+\frac{N_t}{N_b}\frac{d^2\theta}{d\eta^2}=0, \tag{11}$$

$$\left.\begin{array}{l} f(0)=F_A,\dfrac{df(0)}{d\eta}=1,g(0)=-n\dfrac{d^2f(0)}{d\eta^2},\theta(0)=1,\varphi(0)=1 \quad at \quad \eta=0. \\ \dfrac{df(\infty)}{d\eta}\rightarrow 0,g(\infty)\rightarrow 0,\theta(\infty)=\rightarrow 0,\varphi(\infty)=\rightarrow 0 \quad at \quad \eta\rightarrow\infty \end{array}\right\} \tag{12}$$

The emerging parameters in Equation (8)– (12) are defined as:

$$M=\frac{\sigma B_0^2}{\rho A}K=\frac{k}{\mu}\lambda_1=\frac{g\beta_T(T_w-T_\infty)}{b^2x}\lambda_2=\frac{g\beta_C(C_w-C_\infty)}{b^2x}R_d=\frac{4\sigma^*T_\infty^3}{3k^*K}Pr=\frac{\mu C_p}{\alpha}\frac{dQ}{d\eta}=\frac{Q}{b}Le=\frac{\nu}{D_B}Nt=\frac{\tau D_T(T_w-T_\infty)}{\nu T_\infty}Nb=\frac{\tau D_B(C_w-C_\infty)}{\nu}F_A=-2v_1\sqrt{\frac{x}{\gamma b}}$$

Where K is the material parameter, M is the magnetic parameter, λ_1 and λ_2 are buoyancy parameters, R_d is the parameter of thermal radiation, Pr is Prandtl number, Q' is the chemical reaction, Brownian motion is Nb, Nt is the thermophoresis, Lewis number Le and F_A is injection/suction parameter.

3. Solution procedure

The system (8)–(11) along with the boundaries (12) is solved with the shooting method. Besides the other methods such as HPM, FDM which are used numerically, the Runge-Kutta scheme is also very capable. Now introduce the new variables,

$$y_1'=y_2$$

$$y_2'=y_3$$

$$y_3'=\frac{1}{K+1}\left[y_2^2-y_3y_1-y_5K+My_2-\lambda_1y_6-\lambda_2y_8\right]$$

$$y_4'=y_5$$

$$y_5'=\frac{1}{\left(1+\frac{K}{2}\right)}\left[y_2y_4-y_1y_5+K(2y_4+y_3)\right]$$

$$y_6'=y_7$$

$$y_7'=\frac{Pr}{1+Rd}\left[-y_1y_7-Nby_7y_9-Nty_7^2-Q'y_6\right]$$

$$y_8'=y_9$$

$$y_9'=\left[Le(-y_1y_9)-\frac{Nt}{Nb}y'_7\right]$$

The relation in 12 are:

$$\eta=0:\ y_1=F_A,\ y_2=1,\ y_4=-ny_3,\ y_6=1,\ y_8=1,$$

$$\eta\rightarrow\infty:\ y_2\rightarrow 0,y_4\rightarrow 0,y_6\rightarrow 0,y_8\rightarrow 0.$$

Table 1
Comparison of (-f''(0)) skin friction coefficient by varying of *M*.

M	Sohaib et al. [39]	Liaqat et al. [40]	Bagh et al. [41]	Present Results
	$\beta = 0$			
0.0	1.0000130	1.0000078	1.0000080	1.0000130
0.2	1.0954463	1.0954462	1.0954458	1.0954463
0.5	1.2247454	1.2247452	1.2247446	1.2247454
1.0	1.4142180	1.4142142	1.4142132	1.4142180
1.2	1.4832402	1.4832285	1.4832393	1.4832402
1.5	1.5811396	1.5811392	1.5811384	1.5811396
2.0	1.7320516	1.7320515	1.7320504	1.7320516

Table 2
Comparison of the values of $-f''(0)$ by varying of *M*.

M		Mabood and Das [42]	Fazle and Stanford [43]	Bagh et al. [41]	Present Results
		$\beta = 0$			
0		−1.000008	−1.0000084	−1.0000082	1.0000083
1	1.4142135	1.41421356	1.41421353	1.41421363	
5	2.4494897	2.44948974	2.44948963	2.44948985	
10	3.3166247	3.31662479	3.31662463	3.31662454	
50	7.1414284	7.14142843	7.14142839	7.14142835	
100	10.049875	10.0498756	10.0498751	10.0498754	
500	22.383029	22.3830293	22.3830283	22.3830285	
1000	31.638485	31.6384850	31.6384833	31.6384844	

Table 3
The skin friction coefficient by varying *K* and *m*.

N	K	Nazar et al. [44]	Fauzi et al. [45]	Pal et al. [46]	Present Results
0	0	−1.0000	−1.0000	−1.0000	−1.0000
	1	−1.3679	−1.3680	−1.3679	−1.3678
	2	−1.6213	−1.6225	−1.6213	−1.6220
	4	−2.0042	−2.0075	−2.0042	−2.0072
0.5	0	−1.0000	−1.0000	−1.0000	−1.0000
	1	−1.2247	−1.2248	−1.2247	−1.2246
	2	−1.4142	−1.4159	−1.4142	−1.4151
	4	−1.7321	−1.7381	−1.7321	−1.7378

Table 4
The heat transfer rate $-\theta'(0)$ by varying of *Pr*.

Pr	Bagh et al. [41]	Fazle and Stanford [43]	Ishak et al. [47]	Dulal Pal [48]	Haile et al. [49]	Sohaib et al. [39]	Present Results
	$\beta = 0$						
072	0.8088	0.8088	-	-	-	0.80863	0.80875
1.00	1.0000	1.0000	1.0000	1.0000	1.0004	1.00000	1.00000
3.00	1.9236	1.9237	1.9237	1.9236	1.9234	1.92367	1.92375
10	3.7207	3.7207	3.7207	3.7207	3.7205	3.72066	3.72061
100	12.2940	-	12.2941	12.2940	12.2962	12.29405	12.29404

It is required to guess four unknown conditions, let $y_3(0) = a, y_5(0) = b, y_7(0) = c, y_9(0) = d$. These conditions are satisfied when $\eta \to \infty$.

4. Results and discussion

The solution for radiation and buoyancy effects on MHD micro-polar nano-fluid flow over a stretching/shrinking sheet with heat source has been achieved numerically. Although various discretization schemes are being implemented for the numerical solution of non-linear ODE's such as FDM, FEM, FVM, etc. yet these techniques are laborious and costly, it is better to use them for complex and irregular domains. In the case of regular domains, the classical Runge-Kutta method is a reliable technique for the solution of ODEs. It is one of the widely used procedures, it is cost-effective, it can be easily coded and it provides an accuracy of five places of decimal. The quantities (velocity, nanoparticle volume fraction, temperature and micro rotation, skin friction factor, and Nusselt number) are

Table 5
Results for $-f''(0)$ and $-g'(0)$.

M	K	$-f''(0)$[50]	$-f''(0)$[39]	Our Results	$-g'(0)$[50]	$-g'(0)$[39]	Present Results
0.0	0.2	0.909698	0.909798	0.909792	0.094995	0.094895	0.094893
0.5		1.114368	1.114378	1.114374	0.105085	0.105088	0.105081
1.0		1.287147	1.287148	1.287146	0.112058	0.112048	0.112045
	0.0	1.414208	1.414228	1.414224	0.000000	0.000000	0.000000
	0.5	1.140781	1.140772	1.140778	0.211157	0.211165	0.211169
	2.0	0.769749	0.769755	0.769752	0.358659	0.358646	0.358644

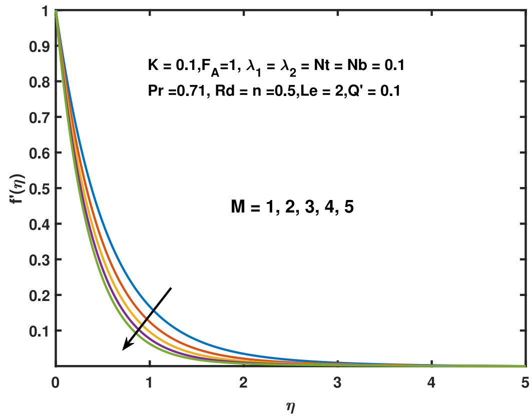

(a)

Fig. 2. Plot for velocity profile $f'(\eta)$ with varying values of M.

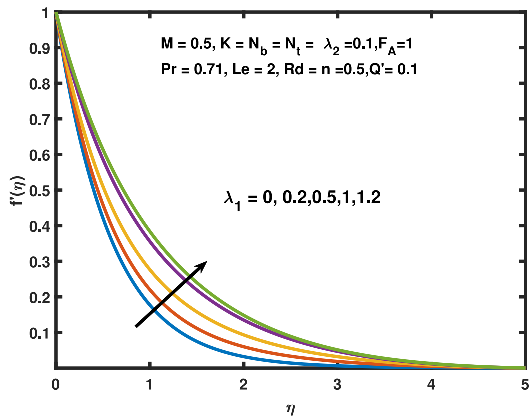

(a)

Fig. 3. Plot for velocity profile $f'(\eta)$ with varying values of λ_1.

evaluated to reveal physical insight. The governing parameters are varied in suitable ranges during that computational procedure. Plots of representative outcomes are exposed. From Table 1, it is obvious that with the boosting values of M, there is an increment in the skin friction factor. An acceptable accord of outcomes with those of Sohaib et al. [39], Liaqat et al. [40] and Bagh et al. [41] testify the validity of our results. In Table 2, it can be seen that enrichment in the value of M causes an increase in the $-f''(0)$ as presented by Mabood and Das [42], Fazle and Stanford [43], and Bagh et al. [41]. Table 3 shows the comparison results for skin friction with [44–46]. It is observed that the increasing values of K and n causes decreasing in skin friction coefficient. Table 4 shows the results for heat transfer rate obtained by using the Runge-Kutta method and the previous results in Refs. [39,41,43,47–49]. It is observed that with the enrichment in the values of Pr, the values of $-\theta''(0)$ is increased. In Table 5, it is apparent that there is an increase in $-f''(0)$

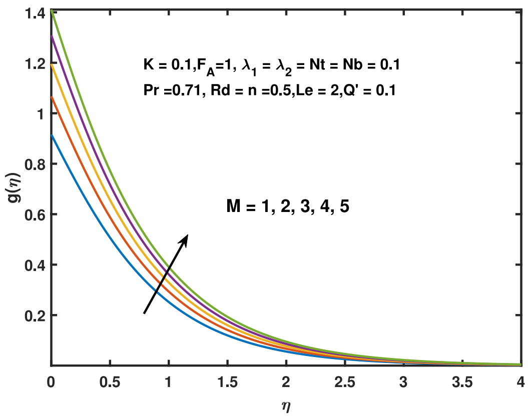

(a)

Fig. 4. Plot for velocity profile $g(\eta)$ with varying values of M.

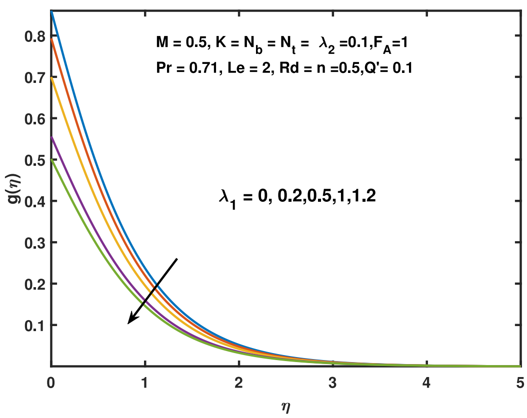

(a)

Fig. 5. Plot for velocity profile $g(\eta)$ with varying values of λ_1.

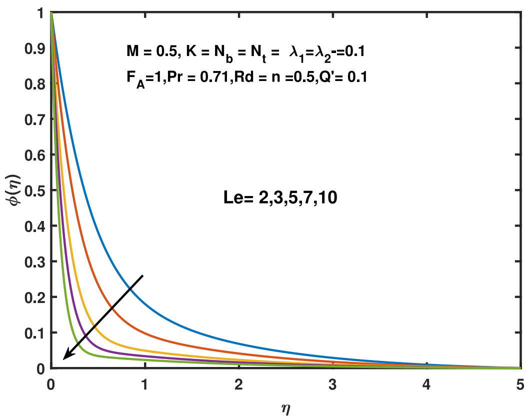

(a)

Fig. 6. Plot for φ with varying values of Le.

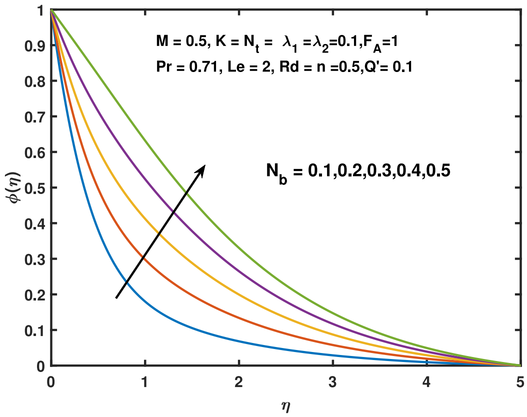

(a)

Fig. 7. Plot for φ with varying values of *Nb*.

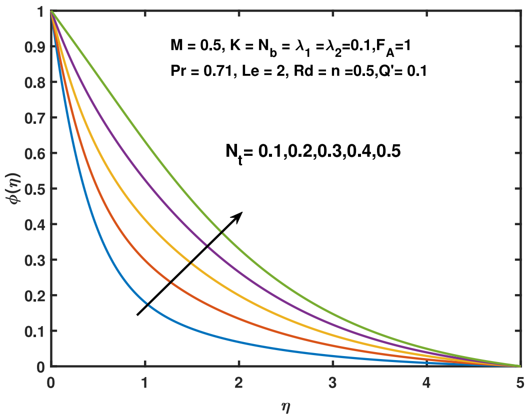

(a)

Fig. 8. Plot for φ with varying values of *Nt*.

and $-g'(0)$ with the increment of K and M, to be compared with the published articles [39,50].

By using the different values of the parameter M, variations of the velocity profile are drawn in Fig. 2. It is observed that the velocity of fluid flow gets decreased with the increase in M. The reason behind is the action of a resistance (Lorentz) force that is developed due to the interaction of electric and magnetic fields. The influence of λ_1 on velocity can be observed in Fig. 3. It is clear that the buoyancy factor increases the velocity.

The buoyancy factor λ_1 (corresponding to the thermal and solutal buoyancy) has accelerated the flow. Fig. 4 portrays the influences of M on micro-rotation $g(\eta)$, it can be seen that there is a clear change in $g(\eta)$ due to magnetic number M. The increase in g can be observed from an enhancement in M because of opposing effect of M to the bulk flow. The buoyancy parameter λ_1 is to decrease $g(\eta)$, as shown in Fig. 5 because there is rapid translatory as well as rotatory motion in micro-polar fluids which causes the decrement in density. Lewis number is a quantity which has no dimension, basically it is a ratio of thermal diffusivity to mass diffusivity. So with the increment of Le the concentration profile decreases as shown in Fig. 6. Important role of Nb on concentration profile as shown in Fig. 7. With the rapid random motion of nano-fluids particles, the concentration profile increases owing to higher values of Brownian motion parameter. The impact of Nt on concentration field is shown in Fig. 8. It is observed that Nt increases the concentration profile. Actually, thermophoresis parameter increases the kinetic energy of the nano-fluids molecule, which cause increment in the concentration profile.

5. Conclusions

The effects of buoyancy and thermal radiation on MHD transportation of micropolar base nanofluid flow over an extending surface are analyzed. The impact of specific parameters is explained graphically and discussed. The notable findings are summarized below:

- Increase in magnetic parameter M causes a reduction in the velocity profile. On the other, hand micro-rotation increases with the increase in magnetic parameter M.
- Velocity profile increases for buoyancy parameters while micro-rotation decreases.
- Solutal concentration decreases with the increase in Lewis number.
- The progressive Brownian motion and thermophoresis both develop the nanoparticle concentration φ higher.

Author statement

Saif Ur Rehman and Amna Mariam: Conceptualization, Methodology, Design Asmat Ullah and Muhammad Imran Asjad: Data curation, Writing- Original draft preparation Bruno A. Pansera, Mohd Yazid Bajuri, Ali Ahmadian: Supervision, Validation of Data-Reviewing and Original draft Ali Ahmadian and Muhammad Imran Asjad: Reviewing and Editing the final version and validation of data.

Declaration of competing interest

The authors declare that they have no known competing financial interests or personal relationships that could have appeared to influence the work reported in this paper.

References

[1] Z. Xie, Y. Jian, Electrokinetic energy conversion of nanofluids in mhd-based microtube, Energy 212 (2020) 118711.
[2] A. Mitra, Computational modelling of boundary-layer flow of a nano fluid over a convective heated inclined plate, JOURNAL OF MECHANICS OF CONTINUA AND MATHEMATICAL SCIENCES 13 (2) (2018) 88–94.
[3] T. Chakraborty, K. Das, P.K. Kundu, Ag-water nanofluid flow over an inclined porous plate embedded in a non-Darcy porous medium due to solar radiation, J. Mech. Sci. Technol. 31 (5) (2017) 2443–2449.
[4] M. Ziaei-Rad, A. Kasaeipoor, M. Mehdi Rashidi, G. Lorenzini, A similarity solution for mixed-convection boundary layer nanofluid flow on an inclined permeable surface, J. Therm. Sci. Eng. Appl. 9 (2).
[5] F. Mebarek-Oudina, Convective heat transfer of titania nanofluids of different base fluids in cylindrical annulus with discrete heat source, Heat Tran. Asian Res. 48 (1) (2019) 135–147.
[6] J. Raza, M. Farooq, F. Mebarek-Oudina, B. Mahanthesh, Multiple Slip Effects on Mhd Non-newtonian Nanofluid Flow over a Nonlinear Permeable Elongated Sheet, Multidiscipline Modeling in Materials and Structures.
[7] K.A. Kumar, V. Sugunamma, N. Sandeep, Influence of viscous dissipation on mhd flow of micropolar fluid over a slendering stretching surface with modified heat flux model, J. Therm. Anal. Calorim. 139 (6) (2020) 3661–3674.
[8] M. Anwar, S. Shafie, T. Hayat, S. Shehzad, M. Salleh, Numerical study for mhd stagnation-point flow of a micropolar nanofluid towards a stretching sheet, J. Braz. Soc. Mech. Sci. Eng. 39 (1) (2017) 89–100.
[9] K. A. Kumar, V. Sugunamma, N. Sandeep, Thermophoresis and brownian motion effects on mhd micropolar nanofluid flow past a stretching surface with non-uniform heat source/sink, Comput. Therm. Sci.: Int. J. 12 (1).
[10] K.A. Kumar, V. Sugunamma, N. Sandeep, S. Sivaiah, Physical aspects on mhd micropolar fluid flow past an exponentially stretching curved surface, in: Defect and Diffusion Forum, vol. 401, Trans Tech Publ, 2020, pp. 79–91.
[11] N.A. Yacob, A. Ishak, I. Pop, Melting heat transfer in boundary layer stagnation-point flow towards a stretching/shrinking sheet in a micropolar fluid, Comput. Fluids 47 (1) (2011) 16–21.
[12] K.A. Kumar, V. Sugunamma, N. Sandeep, A non-fourier heat flux model for magnetohydrodynamic micropolar liquid flow across a coagulated sheet, Heat Tran. Asian Res. 48 (7) (2019) 2819–2843.
[13] S. Kasiviswanathan, M. Gandhi, A class of exact solutions for the magnetohydrodynamic flow of a micropolar fluid, Int. J. Eng. Sci. 30 (4) 409–417.
[14] M. Khan, A. Shahid, M. Malik, T. Salahuddin, Thermal and concentration diffusion in jeffery nanofluid flow over an inclined stretching sheet: a generalized fourier's and fick's perspective, J. Mol. Liq. 251 (2018) 7–14.
[15] K. Anantha Kumar, V. Sugunamma, N. Sandeep, Physical aspects on unsteady mhd-free convective stagnation point flow of micropolar fluid over a stretching surface, Heat Tran. Asian Res. 48 (8) (2019) 3968–3985.
[16] I. Tlili, M. Mustafa, K.A. Kumar, N. Sandeep, Effect of asymmetrical heat rise/fall on the film flow of magnetohydrodynamic hybrid ferrofluid, Sci. Rep. 10 (1) (2020) 1–11.
[17] A.K. Kempannagari, R.R. Buruju, S. Naramgari, S. Vangala, Effect of joule heating on mhd non-Newtonian fluid flow past an exponentially stretching curved surface, Heat Transfer 49 (6) (2020) 3575–3592.
[18] K.A. Kumar, V. Sugunamma, N. Sandeep, Effect of thermal radiation on mhd casson fluid flow over an exponentially stretching curved sheet, J. Therm. Anal. Calorim. 140 (5) (2020) 2377–2385.
[19] S.E. Ahmed, M. Mansour, A. Rashad, T. Salah, Mhd natural convection from two heating modes in fined triangular enclosures filled with porous media using nanofluids, J. Therm. Anal. Calorim. 139 (5) (2020) 3133–3149.
[20] T. Anwar, P. Kumam, W. Watthayu, An exact analysis of unsteady mhd free convection flow of some nanofluids with ramped wall velocity and ramped wall temperature accounting heat radiation and injection/consumption, Sci. Rep. 10 (1) (2020) 1–19.
[21] H.S. Hassan, Symmetry analysis for mhd viscous flow and heat transfer over a stretching sheet, Appl. Math. 6 (1) (2015) 78.
[22] K.A. Kumar, J.R. Reddy, V. Sugunamma, N. Sandeep, Magnetohydrodynamic cattaneo-christov flow past a cone and a wedge with variable heat source/sink, Alexandria engineering journal 57 (1) (2018) 435–443.
[23] S. Nadeem, R.U. Haq, C. Lee, Mhd flow of a casson fluid over an exponentially shrinking sheet, Sci. Iran. 19 (6) (2012) 1550–1553.
[24] B. Ramadevi, K.A. Kumar, V. Sugunamma, N. Sandeep, Influence of non-uniform heat source/sink on the three-dimensional magnetohydrodynamic carreau fluid flow past a stretching surface with modified fourier's law, Pramana 93 (6) (2019) 86.
[25] K.A. Kumar, J.V.R. Reddy, V. Sugunamma, N. Sandeep, Mhd Carreau Fluid Flow Past a Melting Surface with Cattaneo-Christov Heat Flux, 2019, pp. 325–336.
[26] T. Thumma, O.A. Bég, S.R. Sheri, Finite element computation of magnetohydrodynamic nanofluid convection from an oscillating inclined plate with radiative flux, heat source and variable temperature effects, Proc. Inst. Mech. Eng., Part N: Journal of Nanomaterials, Nanoengineering and Nanosystems 231 (4) (2017) 179–194.
[27] S. Aman, I. Khan, Z. Ismail, M.Z. Salleh, A.S. Alshomrani, M.S. Alghamdi, Magnetic field effect on Poiseuille flow and heat transfer of carbon nanotubes along a vertical channel filled with casson fluid, AIP Adv. 7 (1) (2017), 015036.

[28] A. Govindarajan, et al., Radiative fluid flow of a nanofluid over an inclined plate with non-uniform surface temperature, in: Journal of Physics: Conference Series, vol. 1000, IOP Publishing, 2018, 012173.
[29] A. Kumar, V. Sugunamma, N. Sandeep, R. R. JV, Impact of Brownian Motion and Thermophoresis on Bioconvective Flow of Nanoliquids Past a Variable Thickness Surface with Slip Effects, Multidiscipline Modeling in Materials and Structures.
[30] A.C. Venkata Ramudu, K. Anantha Kumar, V. Sugunamma, N. Sandeep, Heat and mass transfer in mhd casson nanofluid flow past a stretching sheet with thermophoresis and brownian motion, Heat Transfer 49 (8) (2020) 5020–5037.
[31] F. Mabood, S. Ibrahim, W. Khan, Effect of melting and heat generation/absorption on sisko nanofluid over a stretching surface with nonlinear radiation, Phys. Scripta 94 (6) (2019), 065701.
[32] M. Rashidi, M. Ali, N. Freidoonimehr, B. Rostami, M.A. Hossain, Mixed convective heat transfer for mhd viscoelastic fluid flow over a porous wedge with thermal radiation, Adv. Mech. Eng. 6 (2014) 735939.
[33] K.A. Kumar, V. Sugunamma, N. Sandeep, M. Mustafa, Simultaneous solutions for first order and second order slips on micropolar fluid flow across a convective surface in the presence of lorentz force and variable heat source/sink, Sci. Rep. 9 (1) (2019) 1–14.
[34] U. Khan, N. Ahmed, S.T. Mohyud-Din, B. Bin-Mohsin, Nonlinear radiation effects on mhd flow of nanofluid over a nonlinearly stretching/shrinking wedge, Neural Comput. Appl. 28 (8) (2017) 2041–2050.
[35] B. Sakiadis, Boundary-layer behavior on continuous solid surfaces: Ii. the boundary layer on a continuous flat surface, AIChE J. 7 (2) (1961) 221–225.
[36] T.R. Mahapatra, A. Gupta, Magnetohydrodynamic stagnation-point flow towards a stretching sheet, Acta Mech. 152 (1–4) (2001) 191–196.
[37] Y.S. Daniel, Z.A. Aziz, Z. Ismail, A. Bahar, F. Salah, Slip role for unsteady mhd mixed convection of nanofluid over stretching sheet with thermal radiation and electric field, Indian J. Phys. 94 (2) (2020) 195–207.
[38] F. Mabood, S. Ibrahim, P. Kumar, G. Lorenzini, Effects of slip and radiation on convective mhd casson nanofluid flow over a stretching sheet influenced by variable viscosity, J. Eng. Thermophys. 29 (2) (2020) 303–315.
[39] S. Abdal, B. Ali, S. Younas, L. Ali, A. Mariam, Thermo-diffusion and multislip effects on mhd mixed convection unsteady flow of micropolar nanofluid over a shrinking/stretching sheet with radiation in the presence of heat source, Symmetry 12 (1) (2020) 49.
[40] L. Ali, X. Liu, B. Ali, S. Mujeed, S. Abdal, Finite element analysis of thermo-diffusion and multi-slip effects on mhd unsteady flow of casson nano-fluid over a shrinking/stretching sheet with radiation and heat source, Appl. Sci. 9 (23) (2019) 5217.
[41] B. Ali, Y. Nie, S.A. Khan, M.T. Sadiq, M. Tariq, Finite element simulation of multiple slip effects on mhd unsteady maxwell nanofluid flow over a permeable stretching sheet with radiation and thermo-diffusion in the presence of chemical reaction, Processes 7 (9) (2019) 628.
[42] F. Mabood, K. Das, Melting heat transfer on hydromagnetic flow of a nanofluid over a stretching sheet with radiation and second-order slip, The European Physical Journal Plus 131 (1) (2016) 3.
[43] F. Mabood, S. Shateyi, Multiple Slip Effects on Mhd Unsteady Flow Heat and Mass Transfer Impinging on Permeable Stretching Sheet with Radiation, Modelling and Simulation in Engineering, 2019.
[44] R. Nazar, N. Amin, D. Filip, I. Pop, Stagnation point flow of a micropolar fluid towards a stretching sheet, Int. J. Non Lin. Mech. 39 (7) (2004) 1227–1235.
[45] E.L.A. Fauzi, S. Ahmad, I. Pop, Flow over a permeable stretching sheet in micropolar nanofluids with suction, in: AIP Conference Proceedings, vol. 1605, AIP, 2014, pp. 428–433.
[46] D. Pal, G. Mandal, Thermal radiation and mhd effects on boundary layer flow of micropolar nanofluid past a stretching sheet with non-uniform heat source/sink, Int. J. Mech. Sci. 126 (2017) 308–318.
[47] A. Ishak, R. Nazar, I. Pop, Boundary layer flow and heat transfer over an unsteady stretching vertical surface, Meccanica 44 (4) (2009) 369–375.
[48] D. Pal, Combined effects of non-uniform heat source/sink and thermal radiation on heat transfer over an unsteady stretching permeable surface, Commun. Nonlinear Sci. Numer. Simulat. 16 (4) (2011) 1890–1904.
[49] E. Haile, B. Shankar, Heat and mass transfer in the boundary layer of unsteady viscous nanofluid along a vertical stretching sheet, Journal of Computational Engineering 2014 (2014), 345153, https://doi.org/10.1155/2014/345153, 17 pages.
[50] L. Ali, X. Liu, B. Ali, S. Mujeed, S. Abdal, Finite element simulation of multi-slip effects on unsteady mhd bioconvective micropolar nanofluid flow over a sheet with solutal and thermal convective boundary conditions, Coatings 9 (12) (2019) 842.